КОЛЛОИДНАЯ ХИМИЯ/CHEMISTRY OF COLLOIDS

DOI: https://doi.org/10.60797/IRJ.2025.154.21

SOL-GEL FABRICATION OF HYDRATED VANADIUM (V) OXIDE AND ANALYSIS OF ITS XEROGEL PROPERTIES

Research article

Hein M.L.[1,] *, Yarovaya O.V.[2], Senina M.O.[3]
[1] ORCID : 0009-0000-6975-2380;
[2] ORCID : 0000-0001-8661-3235;
[1, 2, 3] D.I Mendeleev University of Chemical Technology of Russia, Moscow, Russian Federation

* Corresponding author (heinmyatlwin2468[at]gmail.com)

Abstract

This study investigates the physicochemical properties of a xerogel derived from a highly stable hydrated vanadium (V) oxide sol, employing a range of analytical techniques including X-ray diffraction (XRD), gas adsorption (ASAP), thermogravimetric/differential scanning calorimetry (TG/DSC), and infrared (IR) spectroscopy. It was observed that the specific surface area of the V_2O_5 xerogel increased after heat treatment at 400 °C, but subsequently decreased with further heating to temperatures of 600 °C, 650 °C, and 700 °C. The nitrogen adsorption-desorption isotherm of the V_2O_5 xerogel revealed the presence of mesoporous structures, with pore diameters ranging from 2 to 100 nm, predominantly between 10 and 50 nm. Additionally, the crystallite size of the V_2O_5 powder was found to increase with elevated heat treatment temperatures. Notably, the V_2O_5 phase remained stable after heat treatment up to 700 °C. The infrared spectroscopy results indicated variations in the intensity and position of the absorption bands for the V_2O_5 xerogel across different heat treatment temperatures (400 °C, 600 °C, 650 °C, and 700 °C). Furthermore, the crystallization, melting, and solidification temperatures of the V_2O_5 xerogel were also established.

Keywords: hydrated vanadium (V) oxide sol, xerogel, physicochemical properties.

ЗОЛЬ-ГЕЛЬ СИНТЕЗ ГИДРАТИРОВАННОГО ОКСИДА ВАНАДИЯ (V) И АНАЛИЗ СВОЙСТВ ЕГО КСЕРОГЕЛЯ

Научная статья

Хеин М.Л.[1,] *, Яровая О.В.[2], Сенина М.О.[3]
[1] ORCID : 0009-0000-6975-2380;
[2] ORCID : 0000-0001-8661-3235;
[1, 2, 3] Российский химико-технологический университет имени Д.И. Менделеева, Москва, Российская Федерация

* Корреспондирующий автор (heinmyatlwin2468[at]gmail.com)

Аннотация

В данной работе проведено детальное исследование физико-химических свойств ксерогеля, полученного из высокостабильного гидратированного золя оксида ванадия (V), с использованием различных аналитических методов, таких как рентгеновская дифракция (XRD), газовая адсорбция (ASAP), термогравиметрический и дифференциальный сканирующий калориметр (TG/DSC), а также инфракрасная спектроскопия (ИК). Установлено, что удельная площадь поверхности гидратированного ксерогеля V2O5 увеличивается после термической обработки при температуре 400 °C, после чего наблюдается её снижение при дальнейших повышениях температуры до 600 °C, 650 °C и 700 °C. Исследование изотерм адсорбции-десорбции азота показало наличие мезопористых структур в ксерогеле, с диаметром пор в диапазоне от 2 до 100 нм, с преобладанием пор размером от 10 до 50 нм. Кроме того, отмечено, что размер кристаллитов порошка V_2O_5 увеличивается с повышением температуры термической обработки, при этом фаза V2O5 сохраняет свою стабильность вплоть до 700 °C. Результаты инфракрасной спектроскопии продемонстрировали изменения в интенсивности и позициях поглощающих полос гидратированного ксерогеля V_2O_5 при различных температурах термообработки (400 °C, 600 °C, 650 °C и 700 °C). Обнаружены также температуры кристаллизации, плавления и затвердевания ксерогеля V_2O_5.

Ключевые слова: гидратированный золь оксида ванадия (V), ксерогель, физико-химические свойства.

Introduction

In recent years, vanadium (V) oxide (V_2O_5) has attracted significant attention due to its unique electrical, optical, and catalytic properties. This transition metal oxide exhibits excellent performance in various applications including energy storage (especially in vanadium redox flow batteries), catalysis, sensors, and as a pigment in ceramics and glass. The importance of V_2O_5 in technological advancements necessitates a deeper understanding of its structural properties and how these properties can be manipulated through various synthesis techniques [1], [2], [3]. One promising approach to achieve this is through sol-gel fabrication, which enables the controlled synthesis of V_2O_5 with tunable properties.

The sol-gel method is a versatile and well-established technique that allows for the production of oxide materials at low temperatures. It involves the transition of a system from a high dispersion system 'sol' into a solid 'gel' phase, which can be further processed to obtain powders, thin films, or bulk materials. This method is particularly advantageous for synthesizing complex oxides, as it facilitates homogeneity at the molecular level, leading to materials with desirable characteristics. The sol-

gel process typically consists of several stages, including hydrolysis, condensation, gelation, drying, and thermal treatment, each of which can significantly influence the final properties of the resultant material [4].

The xerogel phase, which is obtained after the drying of the gel, acts as a precursor to the final crystalline phases that form upon subsequent thermal treatment. The thermal treatment temperature, in particular, plays a critical role in determining the phase transitions, crystallinity, surface area, and morphology of the synthesized material, ultimately impacting its functional properties. Understanding how varying thermal treatment temperatures affect the properties of V_2O_5 xerogels is crucial for optimizing their performance for specific applications [5].

V_2O_5 exists in several structural forms, with the most stable being the orthorhombic phase, which is typically achieved through heat treatment [6]. The transition from the amorphous or xerogel state to crystalline V_2O_5 involves several exothermic reactions that can be influenced by the thermal regime employed. This article aims to explore the sol-gel synthesis of V_2O_5, focusing on the analysis of the properties of powders derived from its xerogel at various thermal treatment temperatures. By systematically varying the temperature during the thermal treatment phase, we will investigate how different annealing conditions affect the structural, morphological, and compositional properties of the resulting V_2O_5 powders. In addition to assessing crystallinity and phase identification, a variety of analytical techniques will be employed to characterize the synthesized V_2O_5 powders. These techniques will provide insights into particle size and distribution, surface area, porosity, and thermal stability. The findings from this study will contribute to a more comprehensive understanding of the relationship between the synthesis conditions, particularly thermal treatment, and the resultant properties of V_2O_5 powders. This study is expected to facilitate the design of V_2O_5 materials with tailored properties to optimize their performance in various applications.

Research methods and principles

The following reagents were used in this study: vanadium (V) oxide of analytical grade (MRTU 6-09-6594-70) and hydrogen peroxide (H_2O_2) of special purity grade (GOST-177 88). The sol was synthesized as follows: distilled water was added to a round-bottom flask containing a calculated amount of V_2O_5 powder and was dispersed while stirring. The calculated volume of hydrogen peroxide solution was then added, and the mixture was boiled for 10 minutes. The final product obtained was a hydrated vanadium (V) oxide sol with a dark red color.

The morphology and sizes of the nanoparticles were analyzed using a transmission electron microscope (TEM) LIBRA 200 FE HR (Germany). The morphology of the powder was examined with a scanning electron microscope (SEM) JEOL 1610LV (Japan) at the Center of Collective Use of the D.I. Mendeleev University of Chemical Technology of Russia. The crystallographic structure of the sample was analyzed using powder X-ray diffraction (XRD) DX-2700BH with Cu-Kα radiation. The average crystallite size was calculated using the Selyakov-Scherrer equation.

$$Average\ crystallite\ size,\ D = (k\lambda)/(\beta cos\theta) \quad (1)$$

where k is a coefficient taken equal to 0.94; λ = wavelength of X-ray radiation; Θ is the Bragg angle; β = width of the reflection at half maximum.

Thermal analysis of the powder samples was conducted using TG-DSC research on the STA 449F1 Jupiter® synchronous thermal analysis unit from Netzsch, in an atmosphere of argon gas grade "5.5" (99.9995%). The specific surface area of the xerogel was analyzed using the low-temperature desorption method on a specific surface and porosity analyzer (Micromeritics, USA) at the Center for Collective Uses of the D.I. Mendeleev University of Chemical Technology of Russia.

Main results

The synthesis of $V_2O_5.nH_2O$ sol was conducted following the previously established procedure described above, utilizing a molar ratio of vanadium (V) oxide to hydrogen peroxide of [1]:[30]. The sol concentrations varied from 0.3 to 1.6 wt.%. At concentrations below 0.3 wt.%, the system primarily exhibited a solution with precipitate formation. Conversely, concentrations exceeding 1.6 wt.% resulted in the simultaneous formation of both sol and gel phases. The morphology and electron diffraction patterns of the $V_2O_5.nH_2O$ nanoparticles are illustrated in Figure 1. As depicted, the solid phase consists of nanorods with a thickness of approximately 2 nm, a width ranging from 15 to 25 nm, and a length of 0.3 to 0.8 μm, exhibiting a polycrystalline structure. The colloidal chemical properties of these sols, evaluated at varying concentrations, were thoroughly analyzed in a previous study [5]. A summary of the colloidal chemical properties is presented in Table 1 [5]. In addition to the general properties outlined in Table 1, the relationship between sol concentration and viscosity, as well as the pH dependence on the coagulation threshold, was investigated in the prior study. Notably, a marked increase in sol viscosity was observed at concentrations surpassing 1% by mass. Also indicated that the maximum coagulation threshold occurred at a pH range of approximately 2.45 to 2.75; deviations in either direction from this pH resulted in a decrease in the coagulation threshold due to reduced sol stability [7].

Table 1 - Some of the colloidal chemical properties of the hydrated Vanadium (V) oxide sol

DOI: https://doi.org/10.60797/IRJ.2025.154.21.1

№	Properties	Values
1	The region of concentration of sol that keep the sol's stability	0.3 to 1.6 mass %
2	pH that keep the sol stability	2.35 to 3.6 ±0.2
3	Electro kinetic potential, mV	-26±1
4	The maximum point of optical	378 nm

№	Properties	Values
	density, nm	
5	The rapid coagulation threshold value	0.03 mol/liter $NaNO_3$

Note: based on [7]

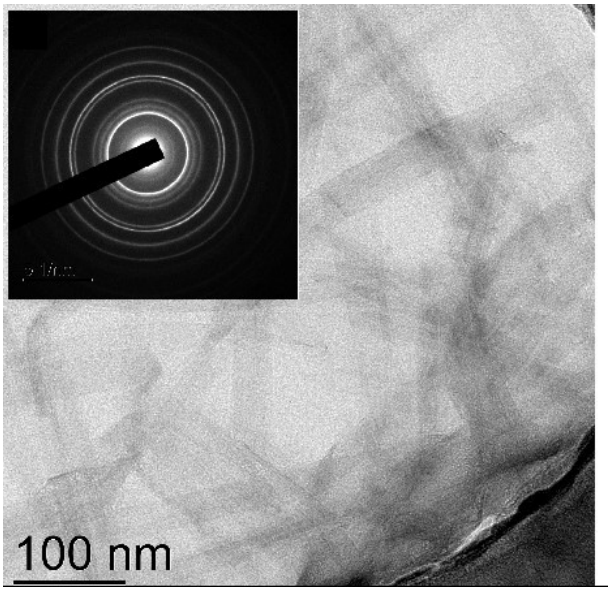

Figure 1 - HRTEM image and electron diffraction pattern of $V_2O_5.nH_2O$ nanorods
DOI: https://doi.org/10.60797/IRJ.2025.154.21.2

To obtain xerogels, sols were dried at room temperature on glass plates. It was observed that during the drying process, the sol formed films. The micrographs of the $V_2O_5.nH_2O$ xerogel film and the samples removed from the glass plate are presented in Figure 2. As shown in this figure 2, the $V_2O_5.nH_2O$ xerogel film exhibits a layered structure composed of overlapping nanorods, resembling the architecture of a wafer. To produce V_2O_5 powder, the dried xerogel was extracted from the plate and subjected to heat treatment in muffle furnace (SNOL 7.2/1300) at a specified temperature for one hour, with a heating rate of 2 °C/min. The resultant micrographs of the V_2O_5 powder after heat treatment at 400 °C, 600 °C, 650 °C, and 700 °C are depicted in Figure 3. Following the heat treatment, the morphology of the powder transitioned to more aggregated forms.

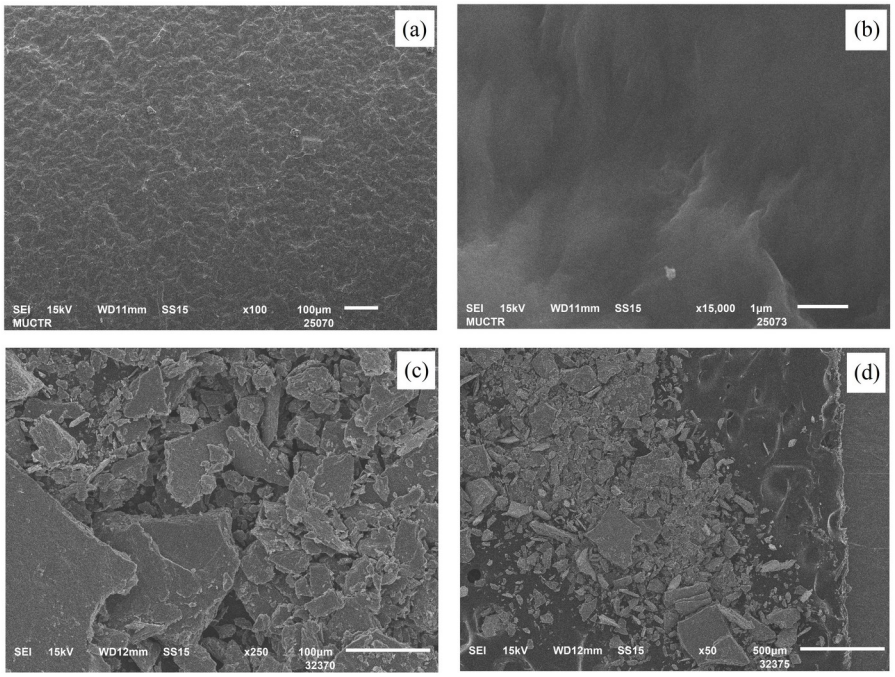

Figure 2 - SEM images of $V_2O_5.nH_2O$ xerogel film (*a*, *b*) on glass plate and (*c*, *d*) after removing from glass plate
DOI: https://doi.org/10.60797/IRJ.2025.154.21.3

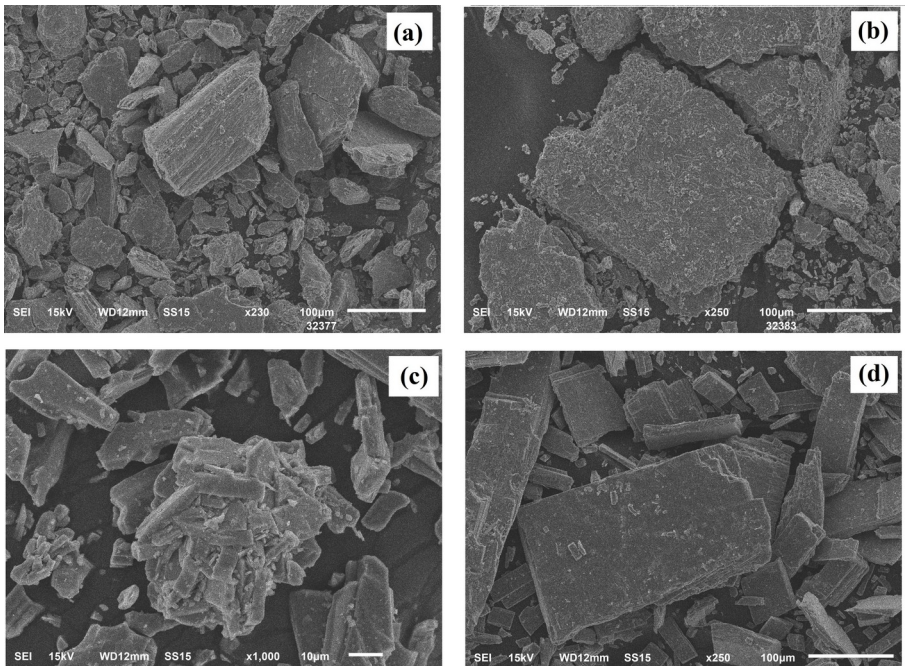

Figure 3 - SEM images of V_2O_5 powder after heat treatment at 400 °C (*a*), 600 °C (*b*), 650 °C (*c*) and 700 °C (*d*)
DOI: https://doi.org/10.60797/IRJ.2025.154.21.4

The results of thermographimetric analysis of $V_2O_5.nH_2O$ xerogel are shown in Figure 4. At the initial stage of heating, the DSC curve shows an endothermic thermal effect "a" of -158.9 J/g accompanied by a mass loss of 6.75%. The effect begins at 99.3 °C, has a peak at 147.6 °C and ends at 169.4 °C. Most likely, it is associated with evaporation of moisture contained in the sample. Upon further heating from 200 to 270 °C, no thermal effects are found on the DSC curve, and with an increase in temperature, two small successive thermal effects "b" and "c" are observed. The endothermic effect begins at 278.7 °C, has a peak at 286.1 °C and ends at 309.4 °C. It has a value of -7.814 J/g and is accompanied by a mass loss of 2.13%. This is due to the partial removal of tightly bound water in the $V_2O_5.nH_2O$ molecule. The exothermic effect "c" begins at 341.7 °C, has a peak at 354.4 °C and ends at 369.7 °C. It has a value of +9.33.2 J/g and is accompanied by a mass loss of 0.71%. This occurs due to the loss of all tightly bound water and crystallization of the material. Upon further heating from 370 to 630 °C, the sample is thermally stable. At 665.1 °C, the melting process of the sample begins, described by the endothermic effect "d" of -212.4 J/g.

This effect has a peak at 674.6 °C, ends at 679.4 °C and is accompanied by a small mass loss of 0.10%. The residual mass of the sample after heating to 791.4 °C was 90.21%.

Cooling begins with the "e" effect, similar to the glass transition effect (inset in the figure). The effect begins at 655.2 °C, has an inflection at 653.7 °C, is in the middle at 653.5 °C, and ends at 651.8 °C. The change value is Cp=0.343 J/(g K). Almost immediately after the "e" effect, the "f" effect begins with a value of 180.3 J/g, corresponding to the solidification process. It begins at 640.9 °C, has a peak at 633.7 °C, and ends at 629.1 °C. No thermal effects were detected during further cooling.

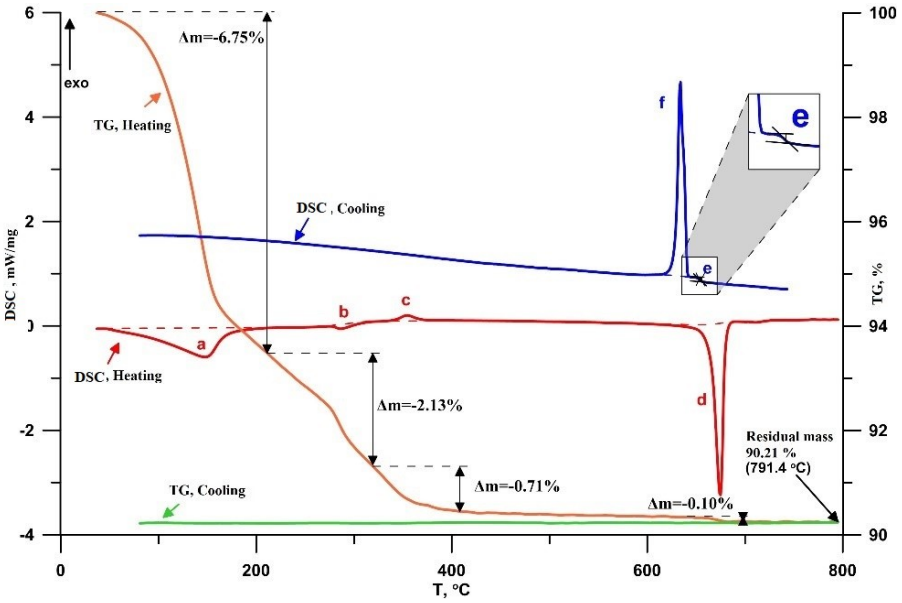

Figure 4 - TG/DSC graph of xerogel $V_2O_5.nH_2O$

DOI: https://doi.org/10.60797/IRJ.2025.154.21.5

It was proved by X-ray diffraction analysis that the particles in the system were $V_2O_5.1.6H_2O$. The diffraction peaks in Figure 5 were in good agreement with the standard X-ray diffraction pattern of $V_2O_5.1.6H_2O$ (JCPDS PDF Card No. 40-1296). The peaks observed at 2θ = 22.7°; 25.54°; 30.49°; 38.50°; 47.07°; 50.55° and 60.30° were assigned to the Bragg reflections (001), (003), (004), (005), (006), (007), respectively. The XRD patterns of powders obtained after heat treatment of $V_2O_5.1.6H_2O$ xerogel at 400 °C/600 °C/650 °C and 700 °C are shown in Figure 6. At the heat treatment temperature of 400/ 600 / 650 and 700 °C, the oxidation state of V_2O_5 does not change according to the V-O phase diagram [8]. The diffraction peaks in Figure 6 were in good agreement with the standard XRD pattern of V_2O_5 (JCPDS PDF Card No. 41-1426). The peaks observed at 2θ = 15.349°; 20.26; 21.72; 26.172; 31.0; 32.364; 33.294; 34.28; 42.0; 45.45; 47.322; 47.84; 52.51; 58.0; 61.07, 62.07; 75.97 and 74.5° were assigned to the Bragg reflections (200), (001), (101), (110), (301), (011), (111), (310), (102), (411), (600), (302), (402), (221), (321), (710), (621), (313), respectively. Some crystal parameters of the obtained samples are shown in Table 1.

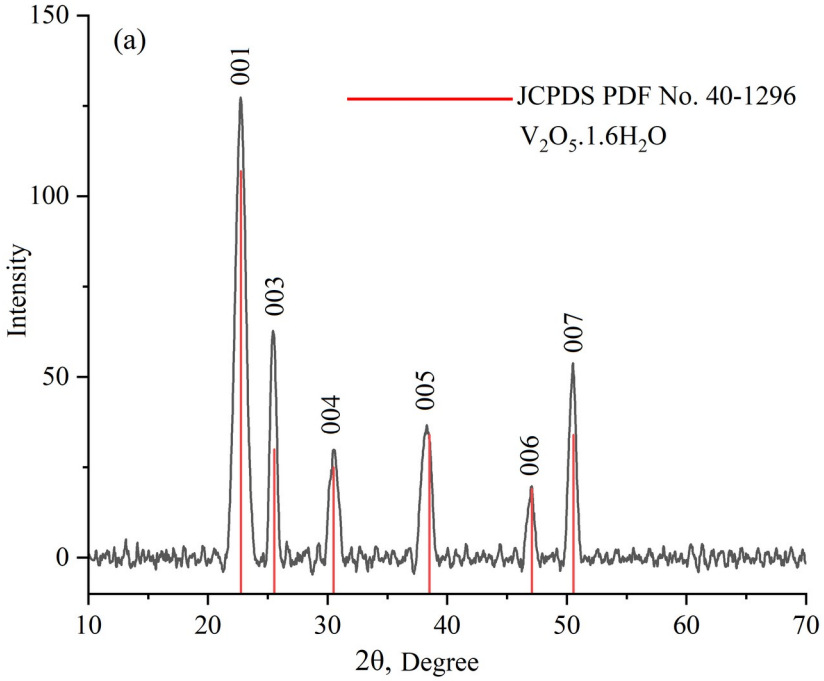

Figure 5 - X-ray diffraction patterns of $V_2O_5.1.6H_2O$ gel obtained after drying the sol at room temperature

DOI: https://doi.org/10.60797/IRJ.2025.154.21.6

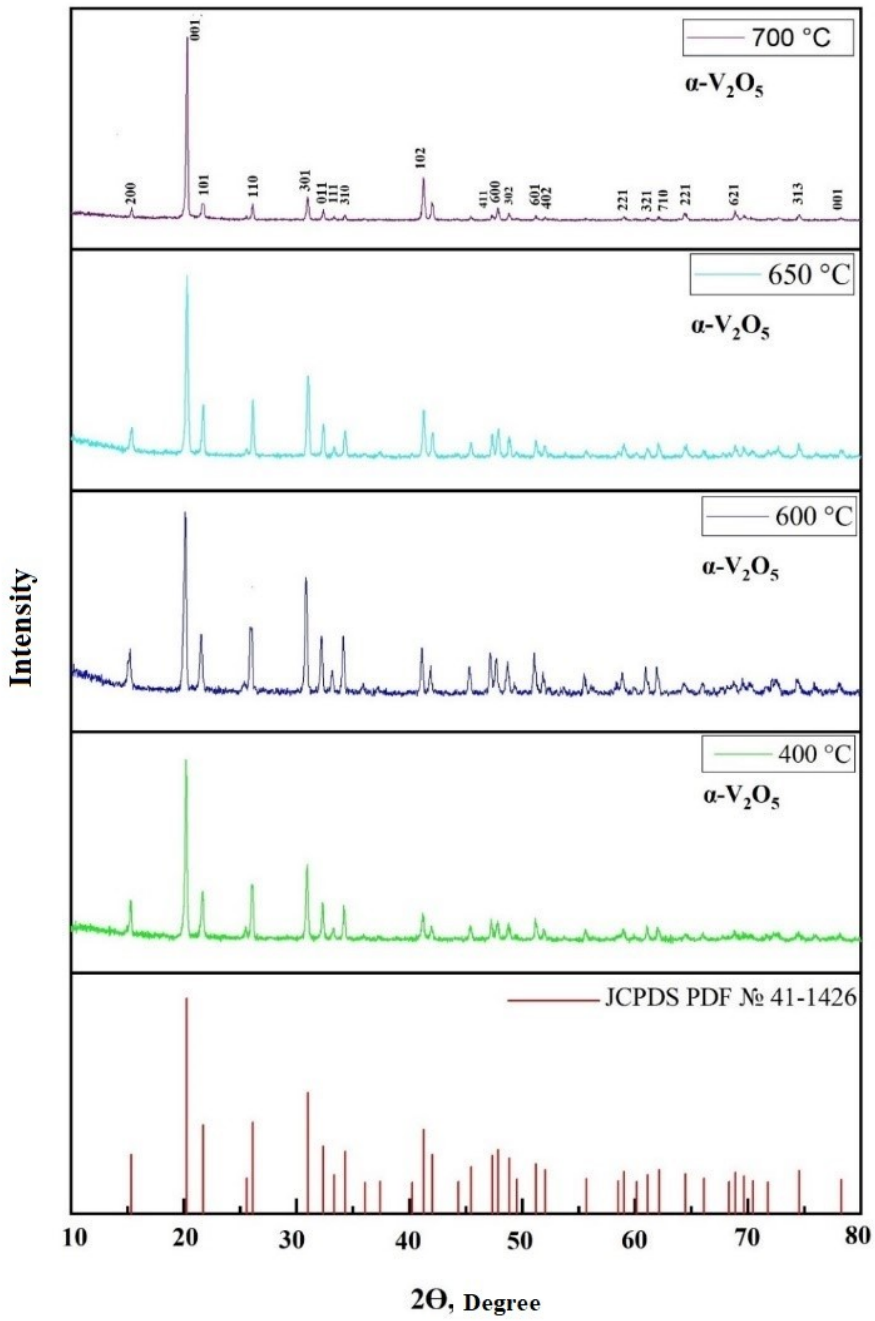

Figure 6 - X-ray diffraction patterns of V_2O_5 powder obtained after heat treatment of $V_2O_5.1.6H_2O$ xerogel at 400 °C / 600 °C / 650 °C and 700 °C one hour

DOI: https://doi.org/10.60797/IRJ.2025.154.21.7

Table 2 - Some crystal parameters of xerogel $V_2O_5.1.6H_2O$ and its powders

DOI: https://doi.org/10.60797/IRJ.2025.154.21.8

№	Heat treatment temperature °C	Average crystallite size nm	Crystal lattice parameters		Crystal system	Phase	JCPDS PDF №
1	Without thermal treatment	~11	a=3,5 Å; b=4,37 Å; c= 11,55 Å	α=90°; β =90°; γ=90°	Orthorhombic	$V_2O_5.1,6H_2O$	40-1296
2	400	~18	a=11,516	α=90°; β		α-V_2O_5	41-1426

№	Heat treatment temperature °C	Average crystallite size nm	Crystal lattice parameters		Crystal system	Phase	JCPDS PDF №
3	600	~18	Å; b=3,5656 Å; c=4,3727 Å	=90°; γ=90°			
4	650	~18					
5	700	~19					

The specific surface area and porosity of the samples were analyzed through low-temperature nitrogen adsorption. The representative isotherms are depicted in Figure 7. Analysis of these isotherms revealed a type IV curve according to the Brunauer classification [9], indicative of polymolecular adsorption. Additionally, the presence of a hysteresis loop suggests capillary condensation within mesopores. This segment of the hysteresis loop corresponds to type H3 in the IUPAC classification [9], indicating the presence of slit-shaped pores. As seen in the images obtained through scanning electron microscopy (Figures 2 and 3), the xerogel exhibits aggregation form of nanorods, creating a layered structure with slit-like pores between the layers.

The adsorption data reveal that when the heat treatment temperature is increased to 400 °C, the specific surface area of the gel increases. This enhancement may be attributed to the removal of water molecules intercalated within the V_2O_5 layers, which reduces layer adhesion and consequently leads to the expansion of the V_2O_5 layers, increasing the surface area of the gel. However, as the heat treatment temperature is elevated further to 600, 650, and 700 °C, a decrease in specific surface area is observed. The specific surface area and porous characteristics of the xerogels subjected to various heat treatment temperatures are summarized in Table 3, as determined by the low-temperature nitrogen adsorption method.

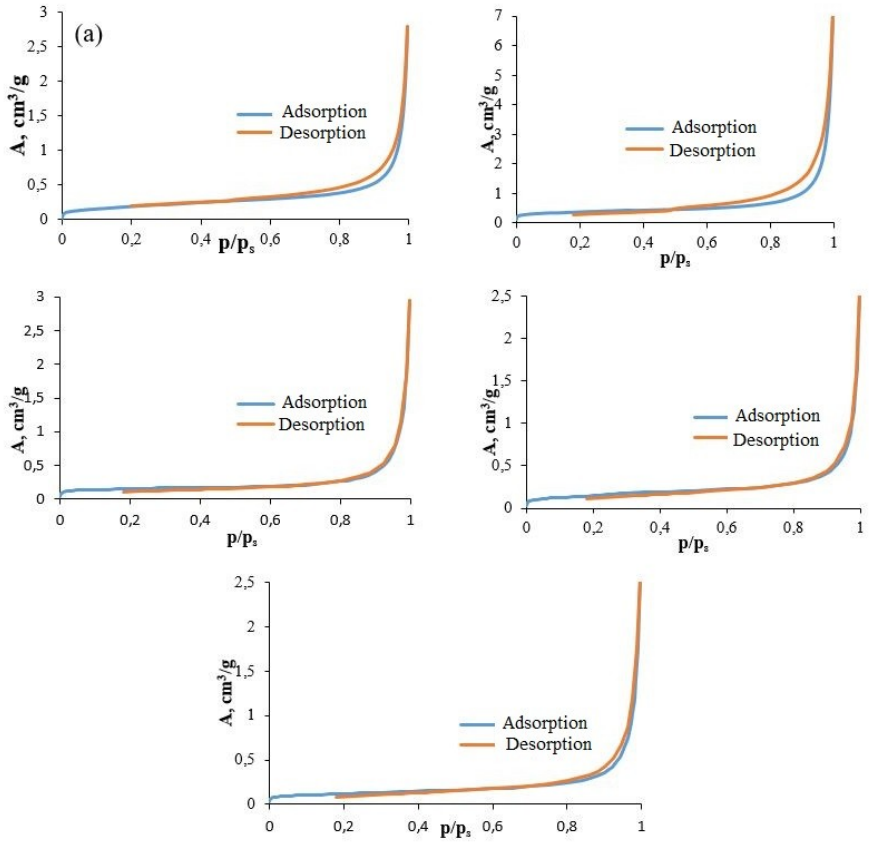

Figure 7 - Adsorption and desorption isotherms of N_2 xerogel $V_2O_5.1.6H_2O$ (*a*) and samples obtained after heat treatment at 400 (*b*) /600 (*c*) /650 (*d*) /700 °C (*d*)

DOI: https://doi.org/10.60797/IRJ.2025.154.21.9

Figure 8 presents the infrared (IR) absorption spectra of xerogels obtained after drying at room temperature and following various heat treatment temperatures. The spectral peaks were identified in accordance with existing literature [10]. The IR spectrum of the $V_2O_5.1.6H_2O$ xerogel features an absorption peak around 3400 cm^{-1}, which corresponds to the deformation vibrations of O–H bonds in the molecular structure. Additionally, a peak near 1620 cm^{-1} is associated with the vibrational modes of water molecules. Weak peaks at approximately 1010 cm^{-1} indicate the presence of short V=O bonds. The absorption peak located at 920 cm^{-1} characterizes the hydrogen bonding between water molecules and the vanadium oxide lattice (V–

O···H). Peaks around 758 cm^{-1} and 407 cm^{-1} correspond to the asymmetric and symmetric stretching vibrations of bridging bonds (V–O–V) within the vanadium-oxygen octahedra, respectively.

Upon subjecting the xerogel to heat treatment at 400 ºC, the IR spectrum reveals a notable decrease in the intensity of the bands associated with water, along with modifications in the intensity and positioning of the bands related to V–O vibrations. These changes reflect the structural alterations in the material as water is evaporated. As the heat treatment temperature is further increased, there is a reduction in the intensity of the V–O vibration bands, which can be attributed to a decrease in the surface area.

Table 3 - Porous characteristics of $V_2O_5.1.6H_2O$ xerogel at different heat treatment temperatures

DOI: https://doi.org/10.60797/IRJ.2025.154.21.10

№	Temperature °C	BET Specific surface area, m^2/g	BJH average pore diameter, nm	BJH desorption pore volume, cm^3/g
1	Without thermal treatment	0,6861	25,5216	0,004339
2	400	1,2731	30,1893	0,011036
3	600	0,5793	40,9484	0,004583
4	650	0,5456	30,907	0,003956
5	700	0,4237	30,2722	0,003942

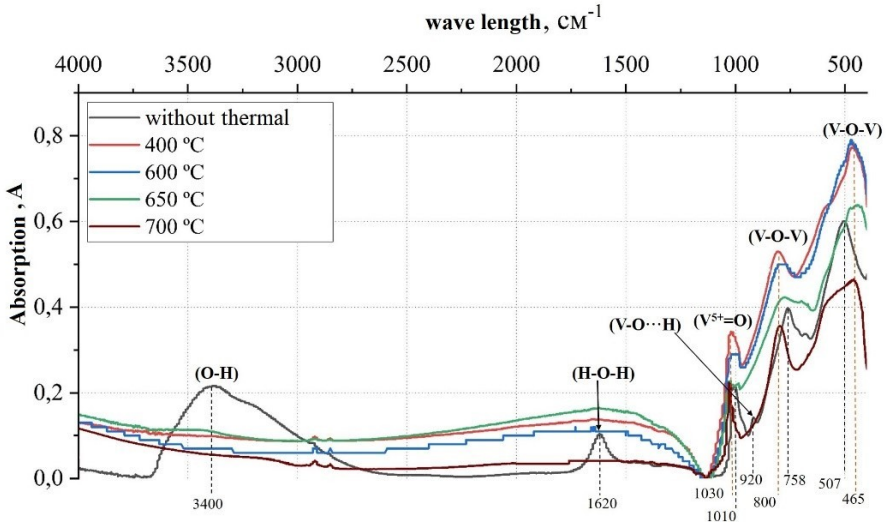

Figure 8 - Infrared spectra of $V_2O_5.1.6H_2O$ xerogel at different heat treatment temperatures

DOI: https://doi.org/10.60797/IRJ.2025.154.21.11

Discussion

In this study, we thoroughly examined the thermal influence on $V_2O_5 \cdot 1.6H_2O$ xerogels derived from a stable hydrated V_2O_5 sol. The dispersion phase, characterized by the formation of nanorods, successfully created a thin film on the glass substrate. X-ray diffraction (XRD) analyses indicated that the xerogels exhibited an orthorhombic crystal structure. Notably, we observed that the crystallite size increased with higher thermal treatment temperatures. Specifically, when the thermal treatment reached 400 °C, the surface area of the xerogels increased, suggesting enhanced texture and porous characteristics. However, further thermal treatment beyond this temperature resulted in a decrease in surface area, indicating possible structural changes or densification that could adversely affect porosity. Additionally, thermogravimetric and differential thermal analyses (TG/DTA) provided critical insights into the melting, crystallization, and solidification points of the material, enhancing our understanding of the thermal stability and transformations occurring within the xerogels. Moreover, infrared (IR) spectroscopy effectively elucidated the molecular structure of vanadium species at various thermal treatment temperatures, contributing to a comprehensive understanding of the phase changes occurring in the material under thermal influence.

Conclusion

The investigation into the thermal influence on $V_2O_5 \cdot 1.6H_2O$ xerogels reveals significant insights into their structural and physical properties. The findings highlight the importance of thermal treatment temperature on crystallite size and surface area, with optimal thermal conditions identified at 400 °C for maximizing surface area. However, further heating beyond this point may lead to undesired structural changes. The integration of XRD, TG/DTA, and IR spectroscopy has proven invaluable in

mapping the thermal behavior and molecular characteristics of vanadium species within the xerogels. This comprehensive study lays the groundwork for future research on the application of V_2O_5 xerogels in various fields, including catalysis and energy storage, where understanding thermal stability and structural integrity is crucial.

Конфликт интересов

Не указан.

Рецензия

Будко Е.В., Курский государственный медицинский университет, Курск Российская Федерация
DOI: https://doi.org/10.60797/IRJ.2025.154.21.12

Conflict of Interest

None declared.

Review

Budko Y.V., Kursk State Medical University, Kursk Russian Federation
DOI: https://doi.org/10.60797/IRJ.2025.154.21.12

Список литературы / References

1. Le T.K. Recent advances in vanadium pentoxide V2O5 towards related applications in chromogenics and beyond: fundamentals, progress, and perspectives. / T.K. Le, P.V. Pham, C.-L. Dong // Journal of Materials Chemistry C. — 2022. — 10. — P. 4019–4071. — DOI: 10.1039/d1tc04872d

2. Xuyan L. V2O5-Based nanomaterials: synthesis and their applications. / L. Xuyan, Z. Jiahuan, Y. Huinan // RSC Adv. — 2018. — 8. — P. 4014–4013. — DOI: 10.1039/C7RA12523B.

3. Sukrit S. 2D van der Waals Oxide with Strong In-Plane Electrical and Optical Anisotropy. / S. Sukrit, Y. Gaihua // ACS Appl Mater Interfaces. — 2017. — 9. — P. 23949–23956. — DOI: 10.1021/acsami.7b05377.

4. Danks A.E. The evolution of ‘sol–gel’ chemistry as a technique for materials synthesis. / A.E. Danks, S.R. Hallb // Mater. Horiz. — 2016. — 91-112. — P. 91–112. — DOI: 10.1039/c5mh00260e

5. Dmitry B. Nanomaterial by Sol-Gel Method: Synthesis and Application. / B. Dmitry, J.A. Turki // Advances in Materials Science and Engineering. — 2021. — 1. — P. 1–21. — DOI: 10.1155/2021/5102014

6. Prze V.-W.M. The Influence of Thermal Conditions on V2O5 Nanostructures Prepared by Sol-Gel Method. / V.-W.M. Prze // Journal of Nanomaterials. — 2015. — 1. — P. 1–18. — DOI: 10.1155/2015/418024

7. Lwin H.M. Colloidal chemical properties of the sol V2O5.nH2O. / H.M. Lwin, O.V. Yarovaya // Nanosystems: Phys. Chem. Math. — 2024. — 15. — P. 487–497. — DOI: 10.1155/2015/418024

8. Wriedt H.A. The O-V (Oxygen-Vanadium) System. / H.A. Wriedt // Bull. AlloyPhase Diagrams. — 1989. — 10. — P. 271–277. — DOI: 10.1007/BF02877512

9. Гаврилова Н.Н. Анализ пористой структуры на основе адсорбционных данных / Н.Н. Гаврилова, В.В. Назаров. — Москва: РХТУ им. Д.И. Менделеева, 2015. — 132 с.

10. Березина О.Я. О механизме внутреннего электрохромного эффекта в гидратированном пентаоксиде ванадия. / О.Я. Березина, П.П. Борисков // Прикладная физика. — 2016. — 3. — С. 85–89. — URL: https://rucont.ru/efd/402096 (дата обращения: 13.04.25).

Список литературы на английском языке / References in English

1. Le T.K. Recent advances in vanadium pentoxide V2O5 towards related applications in chromogenics and beyond: fundamentals, progress, and perspectives. / T.K. Le, P.V. Pham, C.-L. Dong // Journal of Materials Chemistry C. — 2022. — 10. — P. 4019–4071. — DOI: 10.1039/d1tc04872d

2. Xuyan L. V2O5-Based nanomaterials: synthesis and their applications. / L. Xuyan, Z. Jiahuan, Y. Huinan // RSC Adv. — 2018. — 8. — P. 4014–4013. — DOI: 10.1039/C7RA12523B.

3. Sukrit S. 2D van der Waals Oxide with Strong In-Plane Electrical and Optical Anisotropy. / S. Sukrit, Y. Gaihua // ACS Appl Mater Interfaces. — 2017. — 9. — P. 23949–23956. — DOI: 10.1021/acsami.7b05377.

4. Danks A.E. The evolution of ‘sol–gel’ chemistry as a technique for materials synthesis. / A.E. Danks, S.R. Hallb // Mater. Horiz. — 2016. — 91-112. — P. 91–112. — DOI: 10.1039/c5mh00260e

5. Dmitry B. Nanomaterial by Sol-Gel Method: Synthesis and Application. / B. Dmitry, J.A. Turki // Advances in Materials Science and Engineering. — 2021. — 1. — P. 1–21. — DOI: 10.1155/2021/5102014

6. Prze V.-W.M. The Influence of Thermal Conditions on V2O5 Nanostructures Prepared by Sol-Gel Method. / V.-W.M. Prze // Journal of Nanomaterials. — 2015. — 1. — P. 1–18. — DOI: 10.1155/2015/418024

7. Lwin H.M. Colloidal chemical properties of the sol V2O5.nH2O. / H.M. Lwin, O.V. Yarovaya // Nanosystems: Phys. Chem. Math. — 2024. — 15. — P. 487–497. — DOI: 10.1155/2015/418024

8. Wriedt H.A. The O-V (Oxygen-Vanadium) System. / H.A. Wriedt // Bull. AlloyPhase Diagrams. — 1989. — 10. — P. 271–277. — DOI: 10.1007/BF02877512

9. Gavrilova N.N. Analiz poristoi strukturi na osnove adsorbtsionnikh dannikh [Analysis of porous structure based on adsorption data] / N.N. Gavrilova, V.V. Nazarov. — Moscow: D.I. Mendeleev Russian Technical Technical University, 2015. — 132 p. [in Russian]

10. Berezina O.Ya. O mexanizme vnutrennego e'lektroxromnogo e'ffekta v gidratirovannom pentaokside vanadiya [On the mechanism of the internal electrochromic effect in hydrated vanadium pentoxide]. / O.Ya. Berezina, P.P. Boriskov // Applied Physics. — 2016. — 3. — P. 85–89. — URL: https://rucont.ru/efd/402096 (accessed: 13.04.25). [in Russian]